DE-ORBITING SATELLITES IN LEO USING SOLAR SAILS

D. Romagnoli (1), S. Theil (2)
(1) German Aerospace Center, Institute of Space Systems,
Robert Hooke Straße 7, 28359 Bremen, Germany
daniele.romagnoli@dlr.de
(2) German Aerospace Center, Institute of Space Systems
Robert Hooke Straße 7. 28359 Bremen, Germany
stephan.theil@dlr.de

Abstract: Solar sailing is one of the most promising propulsion technologies for future scientific space missions. Although many studies have been performed on solar sails performances and possible applications, successful deploy and use of solar sails in space has been possible only recently, due to the high technological skills and risks involved in developing, packaging and unfolding the sail's booms and the membrane. Hence, the possibility of testing hardware solutions and implementations in space is a key point in order to successfully deploy and operate a solar sail mission in space. In this paper, the use of solar sails as devices to speed up the de-orbiting of LEO objects is considered and the advantage of such approach in the wider context of solar sail development and implementation is discussed.

Keywords: Solar Sail, Mission Design, De-Orbiting.

1 Introduction

The problem of space debris is of crucial interest for the development of future space missions. This is particularly important in Low Earth Orbit, where the high density of both active and inactive satellites makes it vital to prevent collisions between spacecrafts or parts of them. As a consequence, the international community has investigated the problem and defined a set of rules to mitigate this phenomenon. Particularly, in 2006 ASI, BNSC, CNES, DLR and ESA signed a "European Code of Conduct", which defined a set of suggested rules to prevent increasing the amount of space debris in the next years. This document led to the ESA's document "Requirements on Space Debris Mitigation for Agency Projects" on April 2008, which defines the rules to be followed by every future European mission. According to these rules, any European satellite within an altitude of 2000 km has to de-orbit in 25 years after the end of its mission. Hence, meeting this requirement is a driving parameter when designing a new mission in LEO. Possible strategies make use of saved propellant on board to perform a re-entry maneuver at the end of the spacecraft's lifetime, but such an approach is not feasible when the spacecraft has no propulsion system on board. In this case, an alternative solution has to be adopted. Solar sailing represents a promising technology that, however, has yet to be completely proven safe and reliable in space for scientific mission. The recent success of the Japanese Space Agency (JAXA) in deploying and operating a solar sail on an interplanetary journey to Venus clearly demonstrated that solar sailing is a feasible technology of interest for future scientific missions, even though improvements in the technology are still required. However, certifying new hardware solutions in space is not easy because the scientific community believes that today solar sails are not reliable enough for flight. As a consequence, it is mandatory to find alternative and cheap applications in order to test part of the hardware in space. Among the possible ways that can be used to verify different solar sails solutions and configurations, de-orbiting applications using both the atmospheric drag and the solar radiation pressure may represent a preliminary application. Particularly, all the technological processes and solutions involved in the packaging and deployment of the structure, including booms and membrane, may be successfully tested and validated in space. The German Aerospace Center (DLR) has been one of the pioneer research centers to allocate effort in the solar sail technology. As a matter of fact, in 1999 DLR successfully performed an on ground deployment test

of a 20X20 meters square sail (Fig. 1) in the Cologne facility. In recent years, solar sail activities have been pushed back to life and the Gossamer roadmap has been officially presented at the recent 2nd International Symposium on Solar Sailing in New York [1].

Figure 1. The 20-by-20 meters solar sail successfully deployed on ground by DLR in 1999

The first step of the Gossamer project is the deployment of a 5-by-5 meters solar sail in Earth orbit, to demonstrate the capabilities of manufacturing, packaging and successfully deploy in space a fully scalable system (Fig. 2). The evolution with Gossamer-2 will be testing in Earth orbit preliminary attitude and orbit control using the solar radiation pressure as the only source for the required control torques [2, 3, 4]. Finally, a full scale interplanetary mission is intended to be realized as the third step of the program, Gossamer-3. Clearly, the roadmap is challenging and experiences made by other groups all over the world showed that putting a solar sail and successfully deploy it into space is not an easy task: as a matter of fact, the recent unexpected recovery of NanoSail-D2 is a powerful reminder that operating a solar sail in space is not a trivial activity from the technological point of view. As a consequence, the possibility of testing in space complex and sensible mechanisms, such as the deployment system, is of crucial importance in order to achieve the required reliability for more complex scenarios. In this framework, the use of solar sails as aerobraking devices to mitigate the debris problem and reduce the population of potentially dangerous objects in low Earth orbit is an interesting application to test different hardware solutions, even though the solar photon thrust is not properly utilized. This paper examines the possibility of adopting such strategy to test and space qualify techniques and procedures to be adopted in a proper solar sail application. Section 2 is dedicated to the description of the equations of motion that describe the problem and that are used in the simulations. In section 3 the results of the simulations are described and discussed in order to understand what the effect of the solar sail on the orbital and attitude dynamics is. Finally, section 4 summarizes the conclusions of this paper and describes the currently known open points and possible evolutions of this work.

Figure 2. Artistic representation of the Gossamer-1 solar sail in Earth orbit

2. Equations of Motion

Studying the effect of the atmospheric drag on a spacecraft is one of the most challenging activities in simulating the orbital evolution due to the complexity in determining the proper atmospheric density value [5]. However, assuming the adopted atmospheric model is suitable for the desired application, the orbital decay due to the atmospheric drag cannot be studied without introducing the spacecraft attitude dynamics as well. As a consequence, setting up a simulation involves many different aspects to be properly combined without introducing numerical errors or instability in the code[6]. Next subsections describe the dynamical equations used to perform the orbital and attitude propagation.

2.1 Orbital Dynamics

Numerical simulations have been more and more important in determining the orbital evolution of a spacecraft as computer became faster. One of the biggest advantages numerical techniques have against analytical ones is that they allow including any arbitrary disturbing action on the satellite, which may be added to a simple two body problem to better describe the environment the satellite is moving in. This method, known as Cowell's Formulation, makes it possible to express the orbital dynamics as [7]:

$$\ddot{\vec{r}} = -\frac{\mu}{r^3}\vec{r} + \vec{a}_{\text{perturbation}} \qquad (1)$$

being $\vec{a}_{\text{perturbation}}$ the sum of all the disturbing accelerations acting on the spacecraft. As a consequence, it is crucial to properly include and model the perturbations acting on the system in order to achieve a reliable representation of the real world. In the present work, the following perturbations have been considered:

- non spherical gravity field up to J_3;
- gravitational attraction of the Moon and of the Sun, also known as third body effect;
- atmospheric drag;
- solar radiation pressure.

Hence, using the superimposing effect the total perturbation acceleration may be written as:

$$\vec{a}_{\text{perturbation}} = \vec{a}_{\text{grav}} + \vec{a}_{3\text{Body}} + \vec{a}_{\text{drag}} + \vec{a}_{\text{SRP}} \tag{2}$$

2.1.1 Gravitational Perturbation

Since the Earth is not a perfect sphere, the effect of the non symmetric mass distribution has to be taken into consideration using the well established spherical harmonics representation. However, for preliminary purposes, only the more important harmonics and the related accelerations may be considered. In this paper, the non-spherical gravity field of the Earth has been represented up to the J_3 contribution. Given the satellite position $\vec{r} = r_x \hat{i} + r_y \hat{j} + r_z \hat{k}$ in the Earth centered inertial frame, the perturbing accelerations related to these terms may be expressed using well known expressions. The J_2 term describes the oblateness of the Earth and represents the biggest deviation from the spherical gravity field. It may be described as:

$$\vec{a}_{J_2} = -\frac{3 J_2 \mu R_E^2}{r^5} \left\{ \begin{array}{c} \left[1 - 5\left(\dfrac{r_z}{r}\right)^2 \right] r_x \\[2ex] \left[1 - 5\left(\dfrac{r_z}{r}\right)^2 \right] r_y \\[2ex] \left[3 - 5\left(\dfrac{r_z}{r}\right)^2 \right] r_z \end{array} \right\} \tag{3}$$

The J_3 term describes the elliptical shape of the Earth's equator and may be represented by the relation:

$$\vec{a}_{J_3} = -\frac{5}{2}\frac{J_3 \mu R_E^3}{r^7} \left\{ \begin{array}{c} \left[3 r_z - 7 r_z \left(\dfrac{r_z}{r}\right)^2 \right] r_x \\[2ex] \left[3 r_z - 7 r_z \left(\dfrac{r_z}{r}\right)^2 \right] r_y \\[2ex] \left[6 r_z^2 - \dfrac{3}{5} r - 7 \left(\dfrac{r_z}{r}\right)^2 \right] r_z \end{array} \right\} \tag{4}$$

Therefore, the total perturbation coming from the non-spherical shape of the Earth may be approximated by the sum of these three contributions:

$$\vec{a}_{grav} = \vec{a}_{J_2} + \vec{a}_{J_3} \tag{5}$$

2.1.2 Third Body Perturbation

Third bodies, such as the Moon and the Sun, affect the motion of spacecrafts in Earth orbit: the Sun, in fact, is extremely massive, while the Moon is very close. It is important to note that this perturbation becomes more relevant for high altitude orbits, that is when the atmospheric drag effect begins to diminish. The expression for this perturbing acceleration may be derived from the standard three-body problem. Assuming that the mass of the satellite is negligible, one may write:

$$\vec{a}_{3Body} = \mu_3 \left(\frac{\vec{r}_{sat3}}{r_{sat3}^3} - \frac{\vec{r}_{\oplus 3}}{r_{\oplus 3}^3} \right) \tag{6}$$

being μ_3 the gravitational parameter of the third body, $\vec{r}_{sat3}$ is the position vector of the third body with respect to the satellite and $\vec{r}_{\oplus 3}$ is the position vector of the third body with respect to the Earth in the inertial frame. Note that equation (6) may lead to numerical errors when the distance from the satellite to the third body and the distance from the Earth to the third body are very similar: in fact, the cube of these distances appears at the denominator in equation (6), therefore the numerically computed difference is extremely small and may introduce numerical errors in the computation. This problem may be solved using a Taylor series expansion neglecting the small terms [7]:

$$\vec{a}_{3Body} \approx \frac{\mu_3}{r_{\oplus 3}^3} \left[\vec{r}_{\oplus sat} - 3\vec{r}_{\oplus 3} \frac{\vec{r}_{\oplus sat} \cdot \vec{r}_{\oplus 3}}{r_{\oplus 3}^2} - \frac{15}{2} \left(\frac{\vec{r}_{\oplus sat} \cdot \vec{r}_{\oplus 3}}{r_{\oplus 3}^2} \right)^2 \vec{r}_{\oplus 3} \right] \tag{7}$$

It is important to note that even though equation (7) is numerically stable, it is an approximation because the series is truncated. However, it represents a good approximation that can be efficiently used for preliminary analysis.

2.1.3 Atmospheric Drag

Together with the oblateness of the Earth, the atmospheric drag is the most relevant source of perturbing acceleration for LEO satellites. The relation that describes the acceleration due to the atmospheric drag is the well known:

$$\vec{a}_{drag} = -\frac{1}{2} \rho \frac{C_D A}{m} v_{rel}^2 \frac{\vec{v}_{rel}}{\|\vec{v}_{rel}\|} \tag{8}$$

where ρ is the atmospheric density value, C_D is the drag coefficient, A is the projected area in the direction of the velocity vector relative to the atmosphere, m is the total mass of the spacecraft and $\vec{v}_{rel}$ is the velocity of the spacecraft relative to the atmosphere. Assuming the atmosphere is rotating with the Earth and neglecting any wind, the relative velocity may be approximated by the relation:

$$\vec{v}_{rel} = \frac{d\vec{r}}{dt} - \vec{\omega}_{Earth} \times \vec{r} \tag{9}$$

being $\omega_{Earth} = 0.000072921$ rad/sec the angular velocity of the Earth around its spin axis. The key point in computing the atmospheric drag is to determine the atmospheric density value. Different

models are available in the literature, based on both an analytical and an empirical approach, which may lead to remarkably different values of the atmospheric density according to the parameters used to feed the model. In this paper, the Harris-Priester model has been adopted [8]. Even though this is basically a static model, the physical properties of the upper atmosphere in a range between 100 km and 1000 km are computed taking into consideration the solar cycle via tabulated values (Tab. 1). Then, interpolation determines the density at a particular time and altitude. Note that the coefficients in Table 1 correspond to the indices F10.7 = 140 and Ap = 30, according to the predicted values for 2014. Thanks to its computational efficiency, this model is often adopted in early analysis and whenever the simulation requires an estimate of the density value during different phases of the solar cycle. In equation (8), the projected area A represents the connection between the attitude dynamics and the orbital dynamics. As a matter of fact, the atmospheric drag creates a torque acting on the spacecraft that changes its orientation with respect to the inertial frame and, as a consequence, the projected area changes over time and the atmospheric drag acceleration varies during the orbital motion. It is therefore very important to properly simulate the attitude motion in order to accurately predict the acceleration due to the atmospheric drag.

Tab.1 Example of data tables used in the Harris – Priester atmospheric model [7]

Heigth (km)	Minimum Density (kg/m³)	Maximum Density (kg/m³)	Heigth (km)	Minimum Density (kg/m³)	Maximum Density (kg/m³)
100	4.974×10^{-7}	4.974×10^{-7}	420	1.558×10^{-12}	5.684×10^{-12}
120	2.490×10^{-8}	2.490×10^{-8}	440	1.091×10^{-12}	4.355×10^{-12}
130	8.377×10^{-9}	8.710×10^{-9}	460	7.701×10^{-13}	3.362×10^{-12}
140	3.899×10^{-9}	4.059×10^{-9}	480	5.474×10^{-13}	2.612×10^{-12}
150	2.122×10^{-9}	2.215×10^{-9}	500	3.916×10^{-13}	2.042×10^{-12}
160	1.263×10^{-9}	1.344×10^{-9}	520	2.819×10^{-13}	1.605×10^{-12}
170	8.008×10^{-10}	8.758×10^{-10}	540	2.042×10^{-13}	1.267×10^{-12}
180	5.283×10^{-10}	6.10×10^{-10}	560	1.488×10^{-13}	1.005×10^{-12}
190	3.617×10^{-10}	4.297×10^{-10}	580	1.092×10^{-13}	7.997×10^{-13}
200	2.557×10^{-10}	3.162×10^{-10}	600	8.070×10^{-14}	6.390×10^{-13}
210	1.839×10^{-10}	2.396×10^{-10}	620	6.012×10^{-14}	5.123×10^{-13}
220	1.341×10^{-10}	1.853×10^{-10}	640	4.519×10^{-14}	4.121×10^{-13}
230	9.949×10^{-11}	1.455×10^{-10}	660	3.430×10^{-14}	3.325×10^{-13}
240	7.488×10^{-11}	1.157×10^{-10}	680	2.620×10^{-14}	2.691×10^{-13}
250	5.709×10^{-11}	9.308×10^{-11}	700	2.043×10^{-14}	2.185×10^{-13}
260	4.403×10^{-11}	7.555×10^{-11}	720	1.607×10^{-14}	1.779×10^{-13}
280	2.697×10^{-11}	5.095×10^{-11}	760	1.036×10^{-14}	1.190×10^{-13}
290	2.193×10^{-11}	4.226×10^{-11}	780	8.496×10^{-15}	9.776×10^{-14}
300	1.708×10^{-11}	3.526×10^{-11}	800	7.069×10^{-15}	8.059×10^{-14}
320	1.099×10^{-11}	2.511×10^{-11}	840	4.680×10^{-15}	5.741×10^{-14}
340	7.214×10^{-12}	1.819×10^{-11}	880	3.200×10^{-15}	8.059×10^{-14}
360	4.824×10^{-12}	1.337×10^{-11}	920	2.210×10^{-15}	3.130×10^{-14}
380	3.274×10^{-12}	9.995×10^{-12}	960	1.560×10^{-15}	2.360×10^{-14}
400	2.249×10^{-12}	7.492×10^{-12}	1000	1.150×10^{-15}	1.810×10^{-14}

2.1.4 Solar Radiation Pressure Perturbation

Solar radiation pressure is the disturbing action due to the interaction between the photons coming from the Sun and the outer surface of the spacecraft. Even though solar sails rely on this interaction to generate the desired thrust, in low Earth orbit and for the kind of application considered this has to be considered as a perturbation acting on the spacecraft. The solar radiation perturbation may be represented with a relation similar to the one used for the atmospheric drag acceleration:

$$\vec{a}_{SRP} = -\frac{SRP c_R A_{SUN}}{m} \frac{\vec{r}_{sat-Sun}}{\left\| \vec{r}_{sat-Sun} \right\|} \tag{10}$$

being c_R the reflection coefficient, SRP the current value of the solar radiation pressure and A_{SUN} the projected area in the direction of the incoming radiation from the Sun. A detailed description of the model adopted for modeling the solar radiation pressure can be found in [9]. It is important to note that for LEO objects the perturbing acceleration from the solar radiation pressure is several orders of magnitudes smaller than the other disturbing actions. As a consequence, this perturbation plays a minor role in the simulation of the orbital evolution of a low Earth orbit satellite. Note equation (10) shows an intimate connection between the attitude and the orbital dynamics as well: the computation of the projected area in the direction of the incoming solar radiation, in fact, requires the knowledge of the current attitude of the spacecraft. As a consequence, it is crucial to propagate both the attitude and the orbit at the same time in order to properly simulate the problem.

2.2 Attitude Dynamics and Kinematics

Assuming the sailcraft to be a rigid body without internal moving parts, the equations of motion for the attitude dynamics may be easily derived from the standard rotational equation of motion of a rigid body about an arbitrary point [10]:

$$\int \vec{r} \times \ddot{\vec{R}}\, dm = \vec{M}_O \tag{11}$$

where $\vec{r}$ is the position vector of the infinitesimal mass element dm relative to an arbitrary point O, $\vec{R}$ is the position vector of dm in the inertial frame and $\vec{M}_O$ is the total external torque about the point O. After simple math manipulation and under the assumption that the reference point O is either inertially fixed or at the center of mass of the rigid body, the preceding equation may be written as:

$$\dot{\vec{H}}_O = \vec{M}_O \tag{12}$$

being $\vec{H}_O = \int \vec{r} \times \dot{\vec{R}}\, dm$ the angular momentum of the system about the reference point O. The total angular momentum of the system is related to its mass distribution via the inertia matrix of the rigid body about a body fixed reference frame with its origin at the center of mass:

$$\vec{H} = J\,\vec{\omega} \tag{13}$$

Finally, doing the time derivative in equation (12) in the inertial frame, one can prove that the attitude dynamics equation for a rigid spacecraft may be written as:

$$J\dot{\vec{\omega}} + \vec{\omega} \times J\vec{\omega} = \vec{M}_O \tag{14}$$

with proper initial conditions on the angular velocity in the body fixed frame. The attitude propagation is completed with the kinematics equation. The most convenient and numerically efficient way of representing the orientation of a spacecraft is via quaternions. A quaternion **q** is formed by four parameters $(q_1, \quad q_2, \quad q_3, \quad q_4)$ according to the relation [11]:

$$\mathbf{q} \equiv iq_1 + jq_2 + kq_3 + q_4 \tag{15}$$

being i, j and k the hyperimaginary numbers satisfying the following conditions:

$$i^2 = j^2 = k^2 = -1$$
$$ij = -ji = k$$
$$jk = -kj = i \quad\quad (16)$$
$$ki = -ik = j$$

The quaternion in equation (15) may be also seen as made of a scalar or real part, q_4, and a vector or imaginary part, $iq_1 + jq_2 + kq_3$. As a consequence, using the "vector-first" notation, the quaternion **q** may be also represented as:

$$\mathbf{q} = (\vec{q}, q_4) \quad\quad (17)$$

Given the definition of quaternion in (17), the attitude kinematics equation in quaternion notation may be written as follow:

$$\dot{\mathbf{q}} = \frac{1}{2}\Omega\mathbf{q} \qu\quad (18)$$

where Ω is the skew-symmetric matrix computed from the angular velocity vector in the body fixed frame.

3 Simulations Analysis

The simulation of both the orbital and the attitude dynamics at the same time is a challenging numerical task for many reasons. The most crucial one, though, is that they have remarkably different frequencies. As a matter of fact, the orbital motion can be efficiently computed using an integration time step in the order of some minutes, while the attitude has to be propagated at a much higher rate, in the order of at least 10 Hz, to have a good representation of the forces depending on the actual orientation of the spacecraft in case of high angular velocity values. Hence, the integration time step has to be selected to meet the requirements for the attitude propagation, resulting in extremely long computational time. Besides, since the simulated time is usually in the order of years, the second aspect that has to be faced is related to the maximum available memory to store the simulation's data, i.e. state vectors for orbit and attitude, state vectors of the Moon and the Sun and perturbing accelerations. As a matter of fact, during simulations it turned out that MATLAB encountered severe problems in managing memory when the saved files became bigger and bigger thanks to the adopted 10 Hz resolution. Even though sampling the saved data at a lower rate was the easiest way to try coping with this issue, eventually it has been not possible to run simulations longer than several months including the complete attitude and orbital dynamics with high frequency.
The main test case scenario considers the following conditions:

- Orbit: Dawn-Dusk Sun Synchronous Orbit at 620 km altitude
- Total Satellite Mass: 140 kg
- Sail Area: 25 m^2
- Atmospheric Density Model: Harris – Priester

This scenario is consistent with the one adopted for the DLR satellite Asteroid Finder (Fig. 3), which is being presently considered as a candidate mission to test de-orbiting using a solar sail.
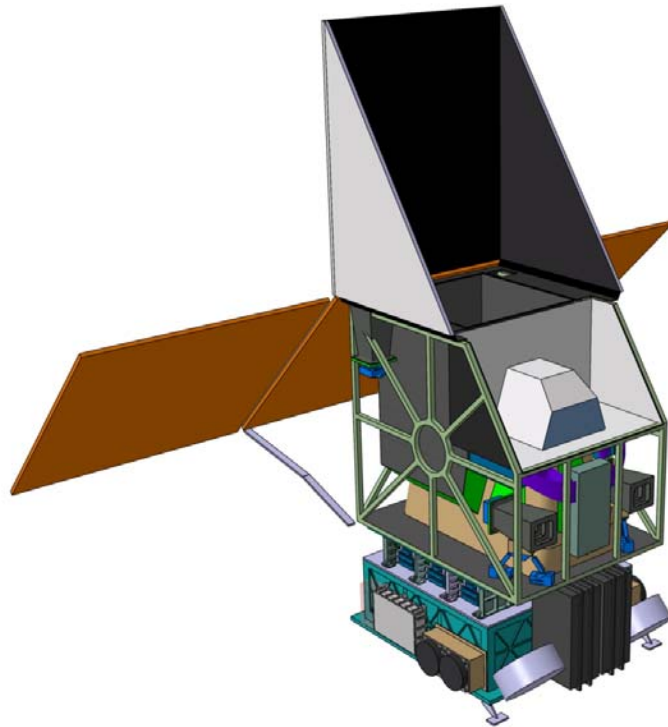
Figure 3. Schematic representation of the current design of the Asteroid Finder satellite

However, in order to check the simulation algorithms avoiding the problems associated with computation time and memory management, a first run has been made with different conditions. Particularly, a lower 450 km circular equatorial orbit has been selected so that a shorter simulation time was required. The preliminary simulation showed that the spacecraft in the test scenario re-enters the atmosphere in approximately three weeks (Fig. 4): note that the vehicle is considered re-entered into the atmosphere when it reaches an altitude of 150 km above the geoid. However, further investigations have to be carried out in a more general framework to determine at which altitude the booms of the solar sail are no longer able to handle the aerodynamic torques, causing the collapse of the structure and defining the altitude at which the sail is not effective any more. Since the attitude has been propagated together with the orbital motion, it is possible to plot the cross section with respect to the atmosphere over time during the simulation (Fig. 5). This information makes it possible to easily visualize the orientation of the spacecraft with respect to the atmosphere: it is clear that the aerodynamic torque acting on the spacecraft is strong enough to provide a passive stabilization, with the sail acting as a parachute and offering a constant area of about 24 m^2 to the rarefied atmosphere. This leads to the best case scenario, where the drag provided by the sail's membrane is maximized for free without any kind of active attitude control thanks to the action of the aerodynamic torque. It is important to note that this passive stabilization might be achieved only if the aerodynamic torque is strong enough. This simulation used an integration time step of one second, that is the attitude dynamics has been sampled at 1 Hz and the associated computation time turned out to be approximately 12 hours. As a consequence, it is easy to imagine that increasing the initial altitude of the spacecraft to the one of the main scenario remarkably increases the simulation time up to unmanageable values.
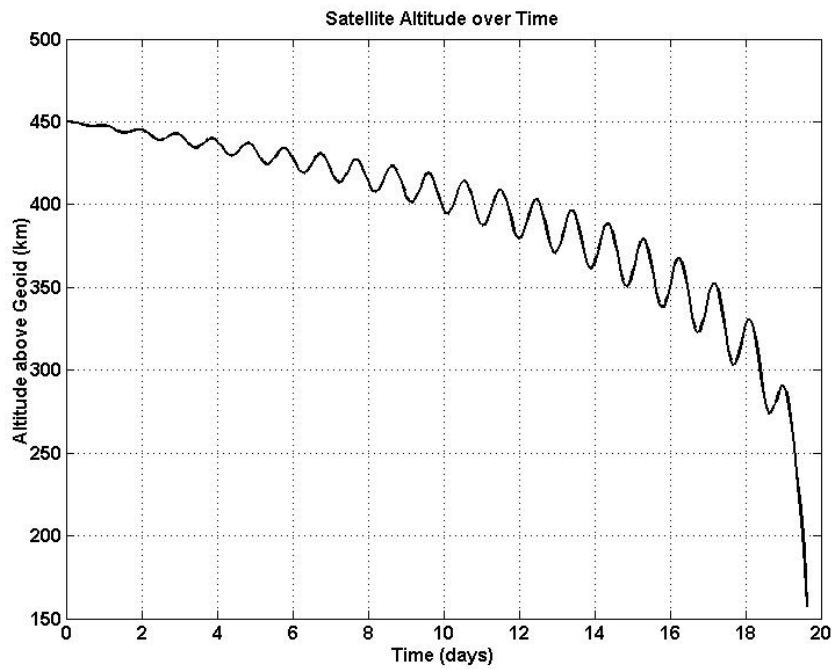
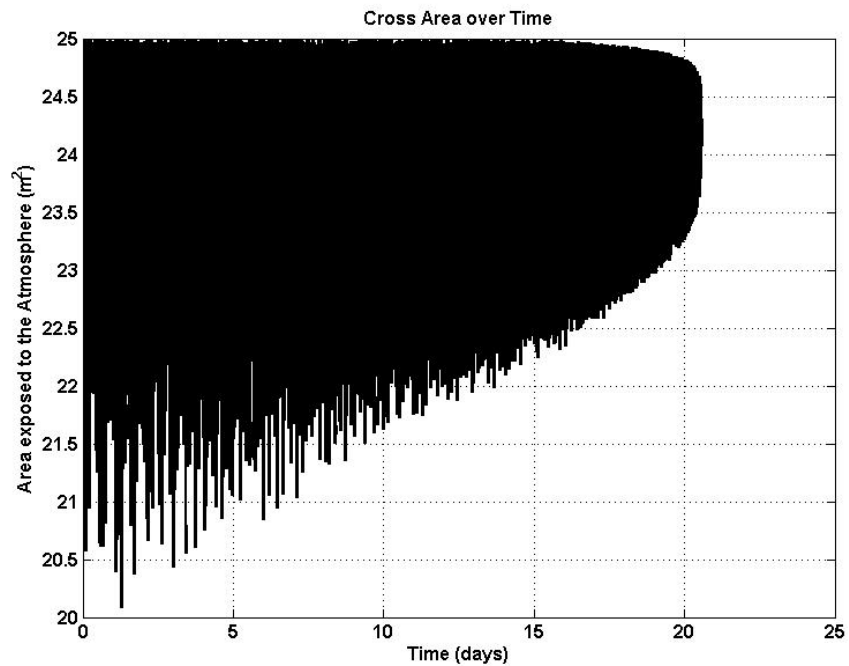**Figure 4. Altitude of the spacecraft over the geoid over time**

Figure 5. Cross area over time

The simulations performed within the main scenario conditions showed that, as expected, also in this case the de-orbiting time might be considerably reduced adopting the sail as an aerobraking device. However, the simulations showed that the desired "passive stabilization" to maximize the area exposed to the atmosphere can not be achieved for the Asteroid Finder-like scenario. This is due to the fact that the available aerodynamic torque is not enough to get rid of the satellite's rotation. As a matter of fact, the atmospheric density is one to two orders of magnitude less at 620 km than at 450 km, resulting in a much smaller drag force according to equation (8). In addition, the peculiar geometry of the Asteroid Finder satellite leads to a center of pressure very close to the satellite's center of mass. The center of pressure, in fact, is located at about seventy centimeters

from the center of mass in the –Y direction of the body fixed frame. As a consequence, the small lever arm combined with the low atmospheric density value lead to a weak aerodynamic torque and to the impossibility of a passively stabilized attitude. Figure 6 shows an example of the cross area over a period of approximately one week: it is clear that the spacecraft tumbles considerably, resulting in a cross section area within the whole range 0 m^2 and 25 m^2.
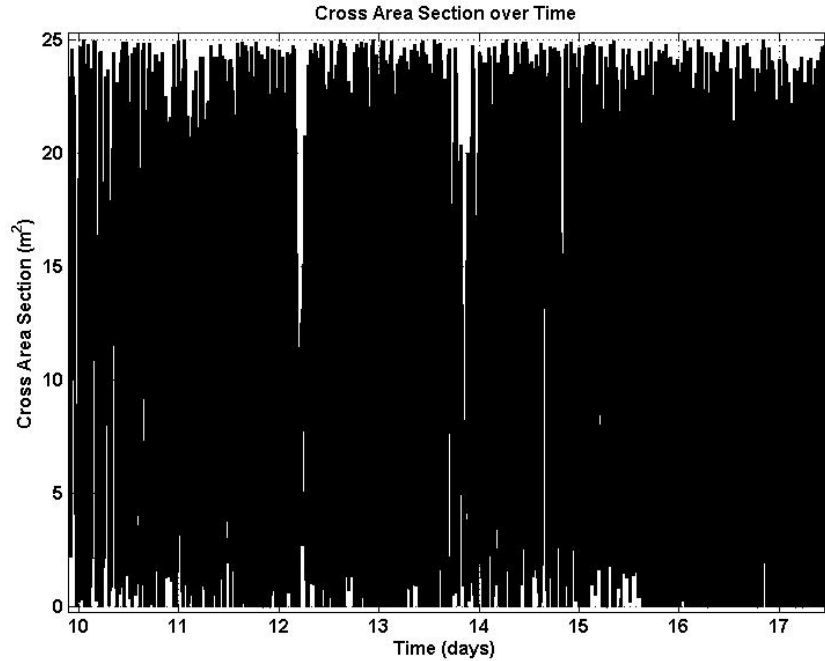

Figure 6. Cross area over time (detailed view of a week timeframe)

Nevertheless, using Tab.1 for computing the atmospheric density, the spacecraft re-enters the atmosphere after approximately 390 days, which is remarkably less than the 9.82 years expected for the Asteroid Finder satellite in the same solar conditions (Fig. 7).
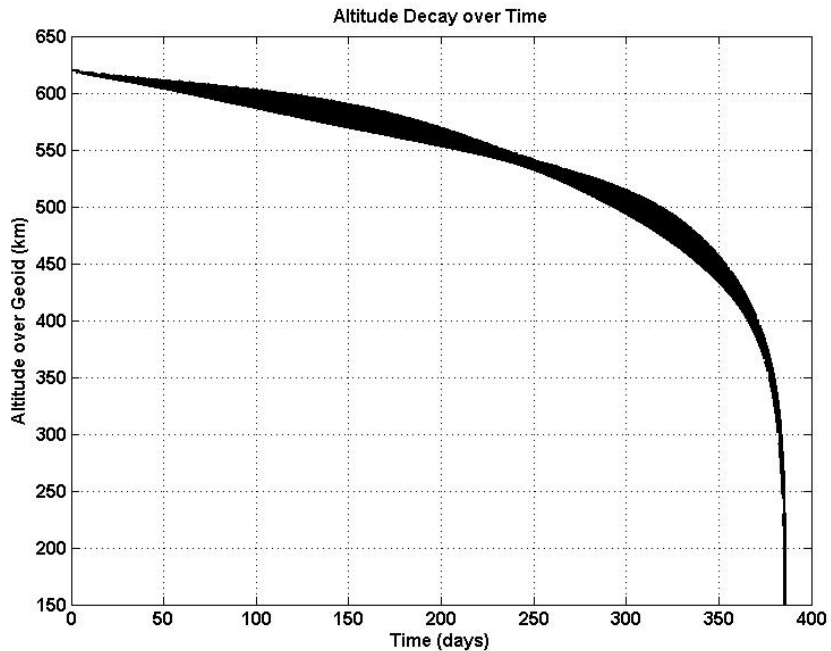

Figure 7. Spacecraft altitude over time for a 620 km SSO orbit

Figure 7 shows the typical atmospheric re-entry behavior: the orbital decay starts extremely slow and constant for most of the time, accelerating remarkably in the last days thanks to the increased atmospheric density value. Hence, the presence of a 5x5 meters solar sail on board a spacecraft like Asteroid Finder represents a big improvement in reducing the danger associated with a dead satellite at the end of its lifetime and allowing to remove a piece of debris from the orbit in a very efficient and affordable way. However, it is important to note that there is a remarkable uncertainty in evaluating the satellite's life time. As a matter of fact, the de-orbiting time may double when the solar flux parameter F10.7 is slightly modified, resulting in much different results. (Fig. 8). Hence, the prediction of the solar activity and of the geomagnetic indexes is extremely important in order to properly evaluate the orbital life time of a spacecraft.
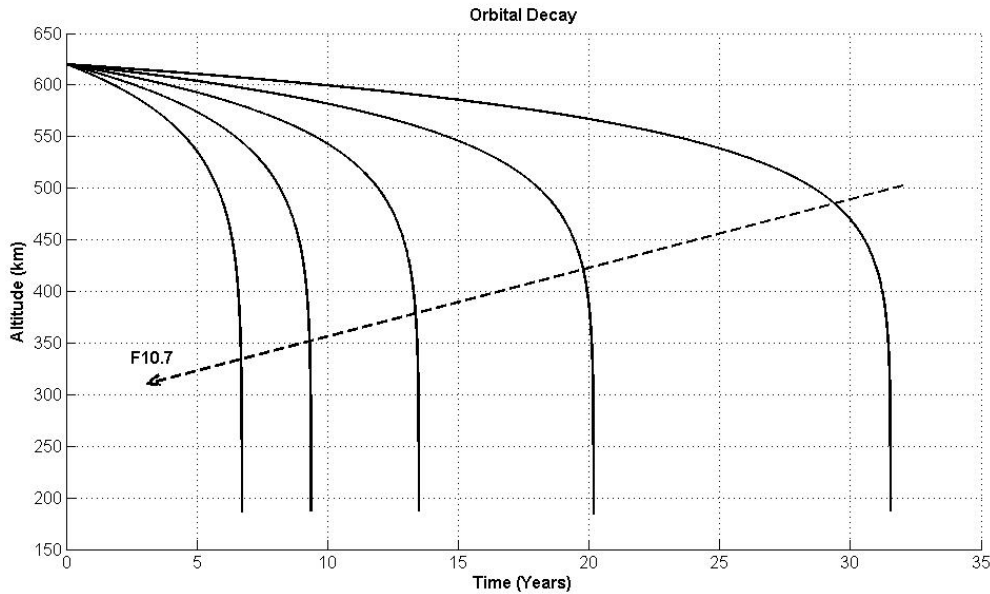

Figure 8. Orbital decay for the Asteroid Finder satellite with different solar F10.7 fluxes

Besides, it is also interesting to note that such strategy may also be adopted not only for satellites natively designed to use a solar sail to de-orbit at the end of lifetime, but also for non cooperative targets. As a matter of fact, the German Space Agency is currently investigating the possibility of rendezvous and docking with a non cooperative spacecraft: in this framework, the use of a cubesat with a deployable solar sail and the ability of chasing and catching a non cooperative target may be successful in removing space debris from LEO or moving GEO satellites to a different orbit without using any propellant but the atmospheric drag or the solar photon trust, respectively.

4 Conclusions

In this paper, the possibility of using a solar sail for de-orbiting spacecrafts in low Earth orbit has been considered. A deep theoretical background associated with the simulation of such an application has been given, as well as a description of the major problems that may occur when facing this task. This preliminary analysis showed that using a small 5x5 meters solar sail can reduce the de-orbiting time up to about 390 days compared to the 9.82 years obtained considering only the external surface of the Asteroid Finder satellite and the same solar flux conditions. Hence, using a solar sail as an aerobraking device may be useful and represent an efficient way of testing in space all the procedures and technical solutions for packaging and deploying the sail's booms and membrane within the framework of a more structured solar sailing developing program. Further investigations have to be carried out to include the structural strength of the sail assembly (boom plus membrane) into account, in order to better understand when the solar sail is not working any

more as a drag device due to the collapse of the structure caused by the aerodynamic torque. In addition, the simulation has been performed neglecting any possible lifting force: as a matter of fact, since the sail's membrane is flying with a certain angle of attack with respect to the atmosphere, the effect of the lift force may extend the lifetime of the spacecraft. However, modeling both the aerodynamic coefficients is not trivial and more detailed experimental data may be required to accomplish this task.

References

[1] Geppert U., Biering B., Lura F. and Reihnard R., "The 3-Step DLR-ESA Gossamer Road Map to Solar Sailing", Proceedings of the 2nd International Symposium on Solar Sailing, New York, USA, 2010.

[2] Romagnoli D. and Oehlschlägel T., "Solar Sail Attitude Control Using a Combination of a Feedforward and a Feedback Controller",Proceedings of the 2nd International Symposium on Solar Sailing, New York, USA, 2010.

[3] Scholz C., Romagnoli D. and Dachwald B., "Performance Analysis of an Attitude Control System for Solar Sails Using Sliding Masses", Proceedings of the 2nd International Symposium on Solar Sailing, New York, USA, 2010.

[4] Romagnoli D. and Oehlschlägel T., "High Performance Two Degrees of Freedom Attitude Control for Solar Sails", Accepted by Advances in Space Research – Special Issue on Solar Sailing, 2011.

[5] Vallado D. A. and Finkleman D., "A Critical Assessment of Satellite Drag and Atmospheric Density Modeling", AIAA/AAS Astrodynamics Specialist Conference and Exhibit 2008, 18-21 August 2008, Honolulu, Hawaii, USA.

[6] Woodburn J. and Tanygin S., " Efficient Numerical Integration of Coupled Orbit and Attitude Trajectories Using an Encke Type Correction Algorithm", AAS 01-428.

[7] Vallado D. A., "Fundamentals of Astrodynamics and Applications – Third Edition", Springer New York, NY.

[8] Montenbruck O. and Gill E., "Satellite Orbits: Models, Methods, Applications", Springer, 2005

[9] McInnes C. R., "Solar Sailing: Technology, Dynamics and Mission Application", Springer, 1999

[10] Wie B., "Space Vehicle Dynamics and Control", AIAA Education Series, 2008

[11] Wertz J.R., "Spacecraft Attitude Determination and Control", Kluwer Academic Publishers, 2002